Analysis of Local Stress Ratio for Delamination in Composites Under Fatigue Loads

Raimondo, Antonio; Bisagni, Chiara

DOI
10.2514/1.J058465

Publication date
2020

Document Version
Final published version

Published in
AIAA Journal: devoted to aerospace research and development

Analysis of Local Stress Ratio for Delamination in Composites Under Fatigue Loads

Antonio Raimondo* and Chiara Bisagni†
Delft University of Technology, 2629 HS Delft, The Netherlands

https://doi.org/10.2514/1.J058465

An approach based on the cohesive zone model for analyzing delamination in composite laminates under cyclic fatigue loading is presented. The proposed technique, called "min-max load approach," is able to dynamically capture the local stress ratio during the progression of delamination. The possibility to know the local stress ratio is relevant in all the situations where its value is different from the applied load ratio and cannot be determined a priori. The methodology analyzes in a single finite element analysis two identical models with two different constant loads, the minimum and the maximum load of the fatigue cycle. The two models interact with each other, exchanging information to calculate the crack growth rate. At first, the approach has been validated in simulations of mode I and mixed-mode propagation using double cantilever beam and mixed-mode bending tests. Then, to prove the effectiveness of the developed methodology, a modified version of the mixed-mode bending test has been analyzed. Mode I and mode II components of the load are decoupled and applied independently, resulting in a local stress ratio different from the applied load ratio. The results obtained from the simulations, compared with the analytical model obtained using the corrected beam theory, show that the proposed approach is able to predict the local stress ratio and thereby to correctly evaluate the crack growth rate during the propagation of the damage.

Nomenclature

a	=	crack length
b_{0I}	=	semi-empirical fatigue delamination growth law exponent
C	=	Paris law constant
d	=	damage variable
d_f	=	fatigue damage variable
d_i^J	=	damage variable at integration point J at cycle i
d_s	=	quasi-static damage variable
G_C	=	critical energy release rate
$G_{\max}$	=	maximum energy release rate in fatigue cycle
$G_{\min}$	=	minimum energy release rate in fatigue cycle
G_{th}	=	energy release rate fatigue threshold
h	=	semi-empirical fatigue delamination growth law coefficient
K	=	cohesive stiffness
l_{CZ}	=	length of cohesive zone
m	=	Paris law exponent
N	=	number of cycles
$P_{\max}$	=	maximum applied load in fatigue cycle
$P_{\min}$	=	minimum applied load in fatigue cycle
R	=	applied load ratio, $P_{\min}/P_{\max}$
R_{Local}	=	local stress ratio, $\sigma_{\min}/\sigma_{\max} = \sqrt{G_{\min}/G_{\max}}$
α	=	function of fracture toughness in semi-empirical fatigue delamination growth law
Δ^0	=	cohesive displacement at damage initiation
Δ^f	=	cohesive displacement at failure
$\Delta d_{\max}$	=	maximum variation of damage variable during a cycle jump
ΔG	=	variation of energy release rate during load cycle
δ^I	=	mode I displacement in modified mixed-mode bending specimen
δ^{II}	=	mode II displacement in modified mixed-mode bending specimen
η	=	Benzeggagh–Kenane material parameter
λ	=	cohesive displacement
τ^0	=	cohesive interface strength
ϕ	=	mixed-mode ratio

I. Introduction

DELAMINATION is one of the most critical types of damage in laminated fiber composites, and it is relevant also in terms of skin-stiffener separation in the case of stiffened structures. It is usually difficult to detect and it can bring severe loss in mechanical properties of the component. Furthermore, it can rapidly grow under the service loading condition, leading to sudden collapse of the structure [1,2].

The estimation of fatigue life of a composite structure remains still a challenge, due to the complexity of the mechanisms involved in the phenomenon. Most of the existing methodologies for the prediction of delamination growth under fatigue loading are based on the Paris law [3]:

$$\frac{da}{dN} = C[\Delta G]^m = C[G_{\max} - G_{\min}]^m \tag{1}$$

where a is the crack length, N is the number of cycles, ΔG is the variation of the energy release rate (G) during the load cycle, and C and m are experimentally determined parameters that depend on the material and on the load conditions. The Paris law, initially developed for fatigue crack evolution in metallic materials, relates the crack growth rate (da/dN) to G. Although ΔG has been widely used to characterize fatigue delamination growth, Rans et al. pointed out in [4] that it can result in an erroneous interpretation of experimental data because it violates the principle of similitude. Based on the analogy with the stress intensity factor variation (ΔK), adopted for fatigue crack growth in metal, the parameter $([G_{\max}]^{0.5} - [G_{\min}]^{0.5})^2$ provides a better characterization of the material behavior. However, for the purpose of this work, ΔG has been considered adequately accurate.

The numerical approaches for the analysis of delamination under fatigue load can be divided in two categories: fracture mechanics and damage mechanics [5]. Fracture mechanics methods are based on the direct application of the Paris law in combination with a procedure for

Presented as Paper 2019-1545 at the AIAA SciTech 2019 Forum, San Diego, CA, 7–11 January 2019; received 14 March 2019; revision received 2 August 2019; accepted for publication 29 August 2019; published online 30 September 2019.

*Post-Doctoral Researcher, Faculty of Aerospace Engineering; a.raimondo@tudelft.nl.

†Professor, Faculty of Aerospace Engineering; c.bisagni@tudelft.nl. Associate Fellow AIAA.

the evaluation of the energy release rate, as the virtual crack closure technique (VCCT) [6–12]. In damage mechanics approaches the degradation of the material interface is described by the evolution of one or more damage variables, and the cohesive zone model (CZM) is adopted to represent the fracture [13–17].

CZM approaches have been widely used in literature for the simulation of interface damage growth under static or impact loading conditions [18–21]. They offer several advantages over the traditional approaches based on fracture mechanics, such as the capability to model damage initiation and overcome the difficulties in the simulation of interface crack between different materials and not self-similar crack growth [22–24]. Lately, CZM have been extended to take into account the effect of cyclic loading by introducing, in addition to the quasi-static formulation, a criterion for the evolution of the damage variable with the number of cycles, which relates the stiffness degradation of the interface to the crack growth rate computed from the Paris law. Usually, for fatigue problems, the CZM approach is implemented together with the “envelope load method” [5], which, instead of simulating the whole variation of the load for each cycle, models only the maximum load of a single cycle. The load variation is taking into account using a predefined parameter, usually the applied (external) load ratio, which is the ratio between the minimum and the maximum applied load during a single fatigue cycle ($R = P_{\min}/P_{\max}$).

The use of the applied load ratio to represent the load variation during the fatigue cycle is one of the main limitations in adopting the envelope load method. Indeed, the crack propagation rate is highly dependent on the local stress ratio, which is the ratio between the minimum and the maximum value of the stress at the crack tip or, alternatively, the square root of the ratio between the minimum and the maximum values of the energy release rate ($R_{\text{Local}} = \sigma_{\min}/\sigma_{\max} = [G_{\min}/G_{\max}]^{0.5}$). Simulating the structure only in the maximum load configuration does not provide any information regarding the deformed shape or the state of stress at the crack tip when the structure is subjected to the minimum load, and then it is not possible to determine the actual value of the local stress ratio.

Hence, for the evaluation of the crack growth rate with the Paris law equation, it is assumed that local stress ratio is equal to the applied (external) load ratio and that it remains constant during the duration of the analysis.

However, the local stress ratio may or may not be equal to the applied (external) load ratio [25] and can change during the damage evolution and along the delamination front. This can happen, for example, when two or more nonsynchronized loads act simultaneously on the structure, when stiffened structures are tested in postbuckling load fatigue conditions, where the buckling mode shape may change between the maximum and the minimum loads of the fatigue cycle, or when the structure oscillates between pre- and postbuckling conditions during the fatigue load [26,27]. In all these situations the local stress ratio is different from the applied load ratio and cannot be predicted in advance. The objective of this work is to develop a methodology based on the finite element (FE) method and on the CZM able to dynamically acquire the local stress ratio along the delamination front and during the evolution of the damage, and shows how the evaluation of this parameter is essential to correctly evaluate the fatigue crack growth rate. In this work, only tension-tension fatigue conditions are considered, because load reversal and negative stress ratio would require additional considerations on the effects of crack closure and contact on delamination propagation.

This paper is organized as follows. In Sec. II, the fatigue damage model based on cohesive element adopted in this work is briefly described, and in Sec. III the theory behind the proposed numerical approach, called “min-max load approach,” and its implementation in the FE code ABAQUS [28] are presented. In Sec. IV the methodology is, at first, validated with results of double cantilever beam (DCB) and mixed-mode bending (MMB) tests taken from literature [8–10], and then applied to a specimen with loading and boundary conditions designed to produce a local stress ratio different from the applied load ratio and can change during the propagation of the damage. Finally, conclusions are reported.

II. Quasi-Static and Fatigue Cohesive Model

Cohesive elements have been developed in the last decades to simulate the initiation and propagation of delamination under quasi-static loading conditions using FE. The cohesive law relates tractions to the separation at the interface where the crack propagation occurs. After an initial elastic part defined by the penalty stiffness, K, the damage initiation displacement (Δ^0) is related to the interfacial strength of the material (τ^0), whereas the final displacement (Δ^f) is defined by the critical energy release rate (G_C), which represents the area under the softening curve (Fig. 1).

The loss of stiffness of the cohesive element is directly related to the evolution of a damage variable (d), which can be calculated from Eq. (2).

$$d = \frac{\Delta^f(\lambda - \Delta^0)}{\lambda(\Delta^f - \Delta^0)} \tag{2}$$

CZM formulation has been extended to simulate also fatigue damage propagation. In this work, the fatigue constitutive model developed by Turon et al. [14] has been adopted. The model of Turon is based on the “envelope load method” and uses the applied load ratio to take into account the load variation. The evolution of the cohesive damage can be expressed for a general loading history as a sum of a component related to the quasi-static damage (d_s) and one related to the fatigue damage (d_f), as shown in Eq. (3):

$$\frac{\partial d}{\partial N} = \frac{\partial d_s}{\partial N} + \frac{\partial d_f}{\partial N} \tag{3}$$

The part related to the quasi-static damage ($\partial d_s/\partial N$) is evaluated according to Eq. (2), whereas the fatigue damage rate ($\partial d_f/\partial N$) defines the evolution of the damage variable as a function of the number of cycles, and, referring to Fig. 1, is formulated as follows:

$$\frac{\partial d_f}{\partial N} = \frac{1}{l_{\text{CZ}}} \frac{[\Delta^f(1-d) + d\Delta^0]^2}{\Delta^f \Delta^0} \frac{da}{dN} \tag{4}$$

where l_{CZ} is the length of the cohesive zone and da/dN is the crack growth rate, defined as a piecewise function using the Paris law:

$$\frac{da}{dN} = \begin{cases} C\left(\frac{\Delta G}{G_C}\right)^m, & G_{\text{th}} < G < G_C \\ 0, & \text{otherwise} \end{cases} \tag{5}$$

where G_{th} is the energy release rate fatigue threshold. The variation of the energy release rate (ΔG) is calculated using the constitutive law and the applied load ratio:

$$\Delta G = G_{\max} - G_{\min} = \frac{\tau^0}{2}\left[\Delta^f - \frac{(\Delta^f - \lambda^{\max})^2}{\Delta^f - \Delta^0}\right](1 - R^2) \tag{6}$$

To avoid a cycle-by-cycle analysis, the model adopts a cycle-jump strategy, considering the number of cycles that can be jumped without expecting any relevant change in the damage state. The damage at each cycle jump is calculated as follows:

$$d^J_{i+\Delta N_i} = d^J_i + \frac{\partial d^J_i}{\partial N}\Delta N_i \qquad \text{with } \Delta N_i = \frac{\Delta d_{\max}}{\max\limits_J\{\partial d^J_i/\partial N\}} \tag{7}$$

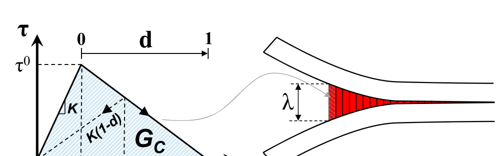

Fig. 1 Constitutive response for traction-separation cohesive elements.

where $d^J_{i+\Delta Ni}$ is the damage variable at integration point J at cycle $N_{i+\Delta Ni}$, d_{iJ} is the damage variable at integration point J at cycle N_i, $\partial d_{Ji}/\partial N$ is the damage rate at integration point J at cycle N_i evaluated using Eq. (4), and ΔN_i is the number of cycle that can be jumped. The cycle jump is evaluated in order to maintain a fixed level of accuracy during the analysis. In particular, it corresponds to the number of cycles that ensure a maximum variation of the damage variable inside the cohesive element layer equal to $\Delta d_{\max}$, which is a fixed parameter defined by the user and represents the sensitivity of the analysis. The smaller the value of $\Delta d_{\max}$ is, the higher is the accuracy of the simulation. As shown in Eq. (7), the cycle jump is calculated, at the cycle N_i, dividing $\Delta d_{\max}$ by the maximum value of the damage rate among all the integration points of the cohesive elements.

III. Min-Max Load Approach

To dynamically capture the local stress ratio it is necessary to have information about the deformed shape of the structure when it is at the minimum and at the maximum load of the fatigue cycle. The idea of the technique developed in this work, called min-max load approach, is to perform a single simulation with two models representing the same structure but with different applied loads. Figure 2 shows the example of a DCB subjected to a sinusoidal load. Instead of analyzing all the fatigue cycles, two identical models are created and analyzed at constant load. One model simulates the deformed shape of the structure when the applied load is equal to the minimum value of the fatigue cycle, and the other one represents the deformed configuration of the specimen at the maximum load. The fatigue calculations, based on the constitutive model described in the previous section, are performed on the model representative of the maximum load configuration, which, instead of using the applied load ratio, takes the value of the energy release rate from the minimum configuration to calculate the local stress ratio and the crack growth rate according to the Paris law equation. On the other hand, the minimum load configuration requires information regarding the damage state in the cohesive layer to update the crack front. These data are exchanged at the beginning and at the end of each cycle jump, as illustrated in Fig. 2.

The proposed approach is implemented in the FE code ABAQUS. The structure is discretized and a mirror copy is performed. This results in two identical FE models subjected to the minimum and the maximum loads, respectively.

To identify the two configurations during the analysis, each element belonging to one configuration has the same number of the corresponding element in the other configuration but with a constant offset (Fig. 3).

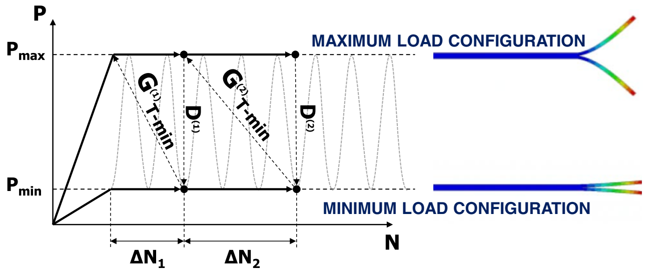

Fig. 2 Min-max load approach.

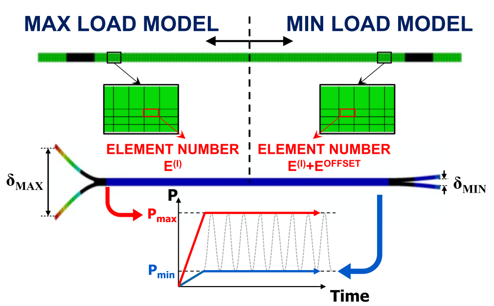

Fig. 3 FE application of min-max load approach.

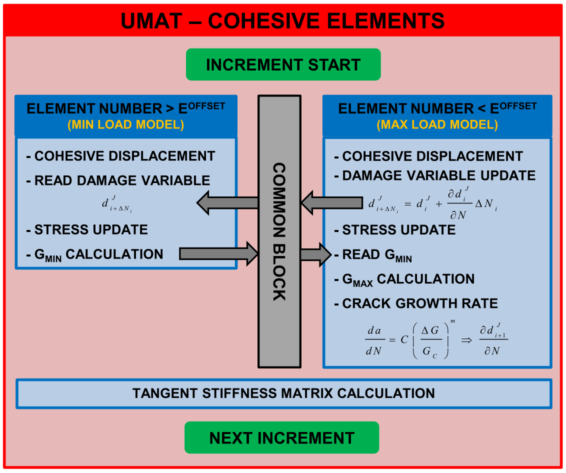

Fig. 4 Fatigue damage model implemented in ABAQUS UMAT subroutine.

The fatigue damage model is implemented by means of a user material subroutine [28] (UMAT). The subroutine, written in Fortran language, is called at each integration point during each load increment of the nonlinear analysis, allowing to define a completely user-defined material behavior. The operations performed inside the developed subroutine are schematically summarized in Fig. 4.

At first, a check is performed to verify if the integration point under consideration belongs to the maximum or minimum load model. In both cases, the nodal displacements provided by the ABAQUS solver are used to evaluate the cohesive element displacement. If the element is part of the structure subjected to the minimum load, then the value of the damage variable is read from the corresponding element of the maximum load configuration, the stresses are updated, and the calculations of the energy release rate are performed. On the other hand, if the integration point under investigation belongs to the maximum load model, then the damage variable is updated together with the stresses, and the fatigue damage calculations are performed using the value of G taken from the corresponding element in the minimum load configuration. Finally, the UMAT requires the definition of the tangent stiffness matrix $(\partial\Delta\sigma/\partial\Delta\varepsilon)$ that is used by the software to improve the convergence rate of the analysis. All information between the two models are exchanged using a COMMON BLOCK, which allows sharing variables between subroutines in the Fortran environment.

IV. Results and Discussion

Numerical simulations have been performed to analyze and validate the response of the developed fatigue approach for crack propagation under pure mode I and mixed-mode condition (I/II) at a different range of the energy release rate. Then, to demonstrate its effectiveness, a numerical investigation has been carried out on a specimen whose boundary and loading conditions are designed to produce a local stress ratio, which can change during the propagation of the damage and is different from the applied load ratio.

A. Simulation of DCB Test

Numerical simulations have been conducted on a DCB specimen to investigate fatigue crack growth under pure mode I loading. The geometrical characteristics and the material properties of the specimen, taken from literature [8], are shown in Fig. 5 and Table 1, respectively.

The two FE models, representing the DCB subjected to the minimum and the maximum loads, are discretized using 2D plane strain elements and four-node cohesive elements with zero thickness. Each arm of the DCB specimen is modeled with three elements through the thickness and, to guarantee an accurate representation of the cohesive process zone, an element length of 0.05 mm is adopted in the propagation region, whereas a coarser discretization is used for

Table 1 Material properties T300/1076

Lamina properties			Interface properties			Fatigue properties		
E_1	[MPa]	139,400	G_{1C}	[kJ/m^2]	0.17	C_I	[mm/cycles]	$2.44\cdot 10^6$
$E_2 = E_3$	[MPa]	10,160	G_{2C}	[kJ/m^2]	0.49	m_I		10.61
$G_{12} = G_{13}$	[MPa]	4,600	η		1.62	G_{th}	[kJ/m^2]	0.06
G_{23}	[MPa]	3,540	τ_3^0	[MPa]	60			
$\nu_{12} = \nu_{13}$		0.30	K	[N/mm^3]	10^6			
ν_{23}		0.436						

the remaining part of the structure. The displacement is applied directly to the nodes at the tip, and the analysis is divided into two steps. In the first quasi-static step, the displacement at each arm tip is increased up to the maximum and minimum values of the fatigue cycle, and only the static damage is taken into account. In the second step, the displacement is kept constant and the fatigue calculation are performed, according to Eqs. (3) and (4).

The deformed shapes of the two structures at the beginning of the fatigue analysis step are shown in Fig. 6, together with enlargements of the crack tip region at the beginning and at the end of the simulation performed at maximum opening displacement of 1.34 mm and applied load ratio $R = 0.1$.

In Fig. 6, the cohesive elements completely damaged are displayed in red, and by comparing the two crack fronts at the end of the fatigue simulation, it is possible to appreciate how the structure subjected to the minimum load keeps track of the crack propagation by acquiring the damage state of each cohesive element from the corresponding element belonging to the structure subjected to the maximum load. As a result, the cohesive zone lengths of the minimum and maximum models are the same between the two models during the whole analysis.

To validate the numerical results, the corrected beam theory (CBT) [29] is adopted to obtain an analytical solution for the problem under consideration. The CBT method starts from the simple beam theory, which considers each arm of the specimen as a linear cantilever beam, but in addition it takes into account shear deformation and local deformation around the crack tip.

According to the linear elastic fracture mechanics theory the energy release rate at the crack tip can be evaluated as follows:

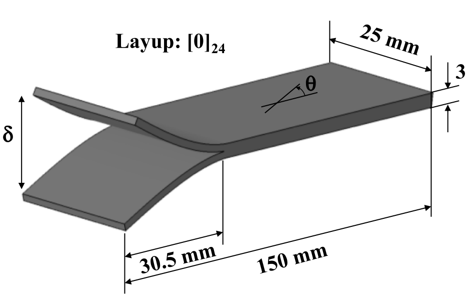

Fig. 5 DCB specimen.

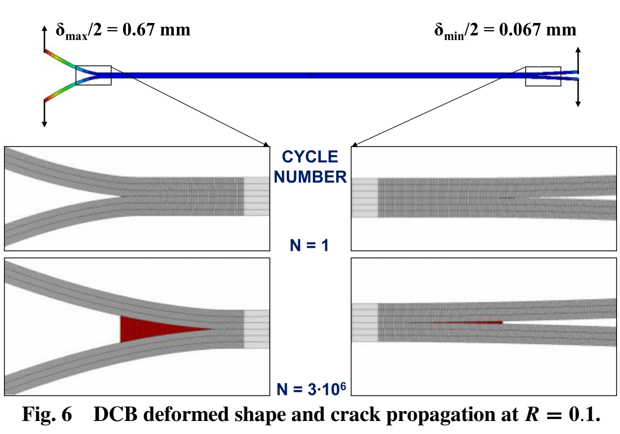

Fig. 6 DCB deformed shape and crack propagation at $R = 0.1$.

$$G = \frac{P^2}{2b}\frac{dC}{da} \tag{8}$$

where P is the applied load, b the width of the specimen, and C is the compliance of the specimen (δ/P), function of the delamination length a. The CBT allows to evaluate the load-displacement relation for the DCB:

$$\delta_I = \frac{2(a+\chi h)^3}{3EI} P_I \tag{9}$$

where P_I is the applied load, δ_I is the opening displacement, h is half of the thickness of the specimen, and $EI = E_{11}bh^3/12$. The coefficient χ represents the correction factor and can be expressed as follows:

$$\chi = \sqrt{\frac{E_{11}}{11G_{13}}\left[3 - 2\left(\frac{\Gamma}{1+\Gamma}\right)^2\right]} \tag{10}$$

with

$$\Gamma = 1.18\frac{\sqrt{E_{11}E_{22}}}{G_{13}} \tag{11}$$

where E_{11} is the longitudinal modulus, E_{22} the transverse modulus, and G_{13} the shear modulus of the composite lamina. From Eq. (9) it is possible to evaluate the compliance of the structure for each value of the delamination length and, solving Eq. (8), obtain a closed-form solution for the energy release rate:

$$G_I = \frac{(a+\chi h)^2}{bEI} P_I^2 \tag{12}$$

The Paris law can now be integrated between the initial delamination length (a_0) and a generic length (a) to evaluate the number of cycles required for the crack to propagate up to that size, as shown in Eq. (13).

$$N = \int_{a_0}^{a} \frac{1}{C\Delta G^m}\,\mathrm{d}a \tag{13}$$

In Fig. 7 the crack length as a function of the number of cycles obtained from the numerical analyses at two values of the applied load ratio is compared with the analytical solution and to the simulation performed, adopting the fatigue crack growth analysis capability available in ABAQUS/Standard. This procedure allows to simulate delamination propagation in a structure subjected to a constant amplitude fatigue load, taking into account for change of contact conditions and geometric nonlinearities. It is based on the direct application of the Paris law using the VCCT equations for the calculation of the energy release rate. A 2D FE model is realized, made of two layers of plane strain elements with coincident nodes along the interface. Each layer is composed of three elements through the thickness while an element length of 0.5 mm is adopted at crack tip and in the propagation area.

The results of the different numerical approaches are in excellent agreement with each other, whereas the small deviations from the analytical predictions are due to the linear formulation of the analytical model.

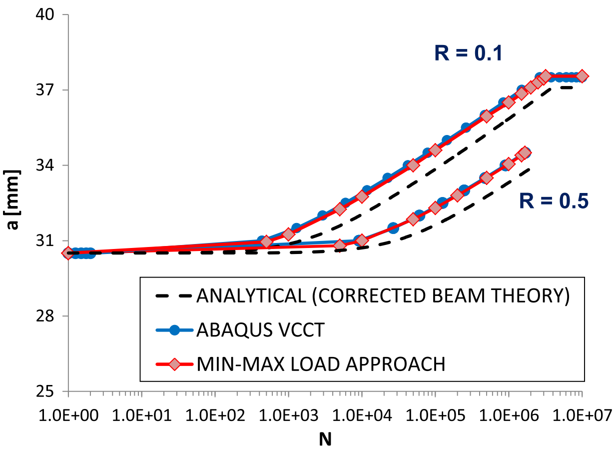

Fig. 7 DCB fatigue crack propagation at different load ratio.

For an applied load ratio equal to 0.1, the delamination length changes from an initial value of 30.5 mm to a final length of 37.5 mm at about 3,000,000 cycles, when the energy release rate at the crack tip is below the threshold value and the crack stops propagating.

The effect of changing the applied load ratio has been investigated by simply increasing the displacement of the minimum load model to half the maximum displacement, resulting in an applied load ratio equal to 0.5. When the load ratio is increased, a reduction of the propagation velocity is obtained, as it can be observed in Fig. 7.

B. Simulation of MMB Test

To investigate delamination propagation in mixed-mode conditions, the MMB test has been simulated taking the specimen data from literature [10]. The geometrical characteristics and the material properties of the specimen with a 20% mixed-mode ratio are shown, respectively, in Fig. 8 and Table 2.

The FE model is realized using the same discretization adopted for the DCB presented in the previous subsection. The load fixture is modeled using rigid beam elements and connected to the structure with multipoint constraints (MPCs). In particular, the front node of the specimen is tied to the lever, whereas for the point in the center, only the relative sliding is allowed. The load is applied by enforcing a prescribed displacement on the loading point of the lever.

The results obtained from the numerical simulation in terms of deformed shape and damage propagation are shown in Fig. 9 for maximum displacement of 1.27 mm and applied load ratio $R = 0.1$.

By observing the deformed crack tip in Fig. 9, it is evident the presence of a sliding component in the opening displacement of the delamination, and, also in this case, it can be noted that the developed algorithm is able to transfer the damage state of the cohesive interface elements between the two models.

As shown in Ref. [30], it is possible to derive an analytical formulation of the problem using the CBT and considering the MMB as a superposition of pure mode I and mode II loadings (Fig. 10).

The total load applied to the lever can be decomposed in pure mode I and mode II loads, according to the length of the lever (c):

$$P_I = \frac{3c - L}{4L} P \qquad P_{II} = \frac{c + L}{L} P \tag{14}$$

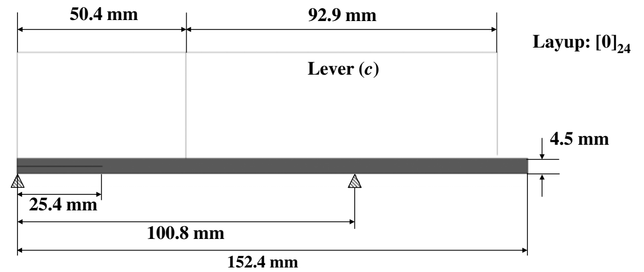

Fig. 8 MMB specimen.

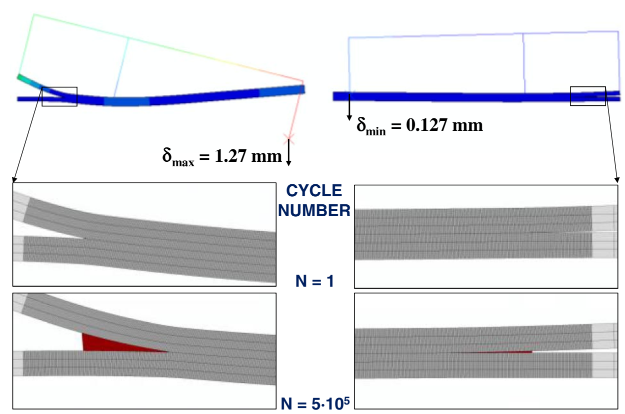

Fig. 9 MMB 20% deformed shape and crack propagation at $R = 0.1$.

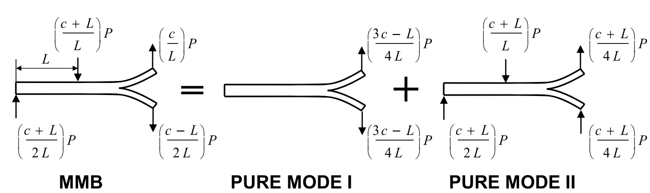

Fig. 10 MMB specimen as a superposition of pure mode I and mode II loadings.

Similarly, also the displacement can be seen as a combination of mode I and mode II displacements:

$$\delta = \frac{3c - L}{4L} \delta_I + \frac{c + L}{L} \delta_{II} \tag{15}$$

Using the CBT it is possible to obtain an equation for the compliance of mode II component:

$$\delta_{II} = \frac{3(a + 0.42\chi h)^3 + 2\,L^3}{96EI} P_{II} \tag{16}$$

The mode II energy release rate can be computed using Eqs. (8) and (16):

$$G_{II} = \frac{3(a + 0.42\chi h)^2}{64bEI} P_{II}^2 \tag{17}$$

Table 2 Material properties IM7/8552

Lamina properties			Interface properties			Fatigue properties		
E_1	[MPa]	161,000	G_{1C}	[kJ/m^2]	0.212	G_{II}/G_T		0.2
$E_2 = E_3$	[MPa]	11,373	G_{2C}	[kJ/m^2]	0.774	$C_{20\%}$	[mm/cycles]	2,412
$G_{12} = G_{13}$	[MPa]	5,200	η		2.21	$m_{20\%}$		8.4
G_{23}	[MPa]	3,900	τ_3^0	[MPa]	60			
$\nu_{12} = \nu_{13}$		0.32	$\tau_1^0 = \tau_2^0$	[MPa]	90			
ν_{23}		0.45	K	[N/mm^3]	10^6			

The total energy release rate of the MMB specimen is the sum of the mode I and mode II components and can be written as follows, using the expressions of the loads in Eq. (14):

$$G_{\text{tot}} = G_I + G_{II} = \left[\frac{(3c-L)^2(a+\chi h)^2}{16L^2bEI} + \frac{3(c+L)^2(a+0.42\chi h)^2}{64L^2bEI}\right]P^2 \quad (18)$$

Substituting the expression of the energy release rate in Eq. (13), the fatigue life of the MMB specimen can be numerically evaluated.

In Fig. 11, the crack length variation as a function of the number of cycles is compared with the results obtained from the VCCT approach implemented in ABAQUS and with analytical solution.

The delamination growth becomes significant around 4000 cycles and then the crack starts to grow steadily. Also in this case, the numerical results obtained using the proposed approach are in an excellent agreement with the results of the VCCT analysis and the analytical predictions.

C. Modified MMB Test

The results of the simulations performed in the previous subsections have shown very good agreement with the analyses performed using the VCCT approach implemented in ABAQUS. Apparently, no advantages are obtained using the min-max load approach because, for the specimens previously considered, the applied load ratio is always equal to the local stress ratio. However, they have been analyzed to prove that the approach is able to simulate the propagation of the delamination and to correctly predict the stress ratio without giving this value as input in the constitutive model.

The min-max load approach has been then applied to a specimen in which the local stress ratio is not equal to the applied load ratio, cannot be predicted in advance, and can change during the propagation of the delamination. To meet these requirements, a modified MMB test has been considered, with the same geometrical characteristics and boundary conditions reported in the previous subsection in Fig. 8 and Table 2. In the classic MMB test, the load or displacement is applied by means of a lever that distributes the load into a mode I and a mode II bending component in a ratio that depends on the length of the lever. In the modified version of the MMB test investigated in this work, the mode I and mode II loads are decoupled from each other and applied separately without using a lever. In particular, a constant mode II displacement (δ^{II}) and a sinusoidal mode I opening displacement, oscillating between the minimum value δ^I_{MIN} and the maximum value δ^I_{MAX}, have been considered, as shown in Fig. 12.

Two identical models have been realized and analyzed in the same analysis at constant load. In particular, one model simulates the behavior of the structure when subjected to the maximum load, which means that a mode I displacement, equal to the maximum value of the displacement during the fatigue cycle (δ^I_{MAX}), is applied together

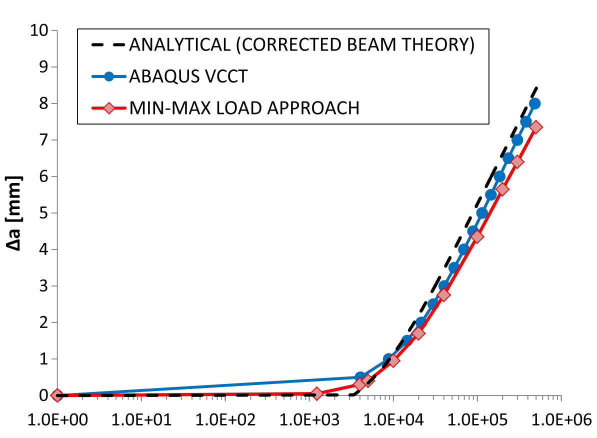

Fig. 11 MMB 20% fatigue crack propagation.

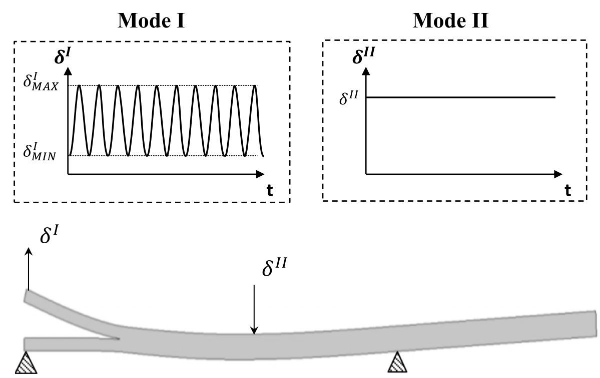

Fig. 12 Modified MMB specimen.

with the mode II displacement (δ^{II}). On the other hand, the model representing the minimum load configuration is characterized by a mode I displacement equal to the minimum value of the displacement during the fatigue cycle (δ^I_{MIN}) and a mode II displacement (δ^{II}) equal to that applied on the maximum load configuration. The two configurations with the boundary and loading conditions are summarized in Fig. 13.

To take into account the variation of the local stress ratio into the constitutive damage model, a semi-empirical fatigue delamination growth law has been adopted in this work. The equation proposed by Allegri et al. [31] and validated using experimental data available in literature describes the effect of mode-mixity and load ratio on the delamination growth rate with a single formula and only three independent material parameters. The adopted fatigue delamination growth law is valid only for positive values of the stress ratio; therefore load reversal is not taken into account in the model. Besides, it is based on the assumption that the stress ratio and the mode-mixity affect only the slope of the fatigue delamination growth rate (da/dN) curve as a function of the normalized energy release rate ($G_{\max}/G_C$), as shown in Eq. (19):

$$\frac{da}{dN} = C\left[\frac{G_{\max}}{G_C(\phi)}\right]^{(b_{0I}/(1-R_{\text{Local}})^{1+\alpha(\phi)})e^{-h\phi}} \quad (19)$$

where ϕ is the mode-mixity ($\phi = G_{II\max}/G_{\max}$) and $G_{\max}$ is the peak value of the energy release rate, defined as the sum of the maximum values of mode I and mode II energy release rate components:

$$G_{\max} = G_{I\max} + G_{II\max} \quad (20)$$

The value $\alpha(\phi)$ is a function of the mode-mixity and of the fracture toughness $G_C(\phi)$:

$$\alpha(\phi) = \frac{G_C(\phi) - G_{IC}}{G_{IIC} - G_{IC}} \quad (21)$$

The mixed-mode fracture toughness can be expressed using the formula proposed by Benzeggagh and Kenane [32]:

$$G_C(\phi) = G_{IC} + (G_{IIC} - G_{IC})\phi^\eta \quad (22)$$

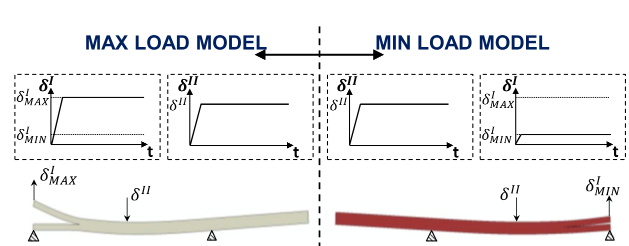

Fig. 13 Min-max load approach for modified MMB specimen.

Table 3 Fatigue coefficients

Material	C, mm	b_{0I}	h
IM7/8552	3.51E − 2	14.05	1.47

Table 4 Applied displacements in modified MMB specimen analyses

δ^I_{MAX}, mm	δ^I_{MIN}, mm	δ^{II}, mm
0.65	0.065	0.05
0.65	0.065	0.10
0.65	0.065	0.15

The factor C, the exponent b_{0I}, and the coefficient h are material-dependent parameters, evaluated using several sets of experimental data on the material IM7/8552 and are reported in Table 3 [31].

Three different simulations have been carried out at different values of mode II displacement (δ^{II}), whereas the fatigue load on mode I component is kept constant with an applied load ratio equal to 0.1 ($R = 0.1$). The aim is to investigate how the addition of a constant load (δ^{II}) during the entire fatigue cycle, from the minimum to the maximum load, affects the local stress ratio and therefore the propagation of the crack. In Table 4 the loading conditions adopted for the three performed analyses are summarized.

The deformed shape obtained by the first analysis is reported in Fig. 14. It can be observed that, even when the fatigue displacement reaches the minimum value, the structure is still loaded due to the presence of the constant displacement δ^{II}.

In Fig. 15 the values of the crack length variation are reported in a function of the number of cycles for all three performed analyses. As expected, increasing the mode II displacement (δ^{II}) leads to higher delamination length due to the increase of the total applied energy release rate.

Once again it is possible to adopt the CBT to obtain an analytical formulation for the problem under consideration. The equations for the modified MMB specimen are similar to those derived for the MMB specimen in the previous subsection. The structure behavior can be represented by a superposition of pure mode I and mode II loadings, but in this case the two components are not related to each other due to the absence of the lever, as shown in Fig. 16.

The total value of the energy release rate can be expressed as the sum of mode I and mode II components, using the equations derived in the previous subsections, as shown in Eq. (23).

$$G_{\mathrm{tot}} = G_I + G_{II} = \frac{(a+\chi h)^2}{bEI}\left(P_I - \frac{P_{II}}{4}\right)^2 + \frac{3(a+0.42\chi h)^2}{64bEI}P_{II}^2 \tag{23}$$

From Eq. (23) it is possible to obtain the minimum and the maximum value of the energy release rate and, then, the local stress ratio. The semi-empirical fatigue delamination growth law, introduced in Eq. (8), can now be numerically integrated between the initial delamination length (a_0) and a generic length (a) to evaluate the number of cycles required for the crack to propagate up to that size, as shown in Eq. (24):

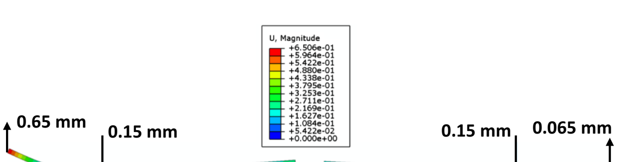

Fig. 14 Modified MMB deformed shape.

$$N = \int_{a_0}^{a} \frac{1}{C[G_{\max}/G_C(\phi)]^{(b_{0I}/(1-R_{\mathrm{Local}})^{1+\alpha(\phi)})e^{-h\phi}}}\,\mathrm{d}a \tag{24}$$

In Fig. 17 the crack length variation as a function of the number of cycles is compared with the analytical solution for all the performed analyses. To prove the effectiveness of the approach proposed in this paper, in Fig. 17 the results are also compared with numerical simulations and analytical solutions obtained without performing the calculation of the local stress ratio. Basically, in these analyses the minimum value of the energy release rate is ignored and it is assumed that the local stress ratio is constant and equal to the applied load ratio ($R_{\mathrm{Local}} = 0.1$), as it is typically done in the current available approaches.

For all the performed analyses, the crack length predicted using the actual value of the local stress ratio is always smaller than the one obtained considering its value equal to the applied load ratio. Indeed, when adding a constant load component to both the minimum and maximum load configurations, the resulting local stress ratio is always larger than the applied load ratio, as schematically shown in Fig. 18, leading to a reduction of the crack growth rate as predicted by the adopted delamination growth law presented in Eq. (19).

Furthermore, from Fig. 17 it is evident that the difference between the results decreases when the mode II displacement is reduced because the value of the local stress ratio decreases and approaches to the applied load ratio. These observations are also confirmed by the graph in Fig. 19, where the local stress ratio, evaluated at the crack tip during the FE analysis, is reported and compared with the values predicted by the analytical model.

It can be observed that the values of the local stress ratio calculated using the min-max load approach are in excellent agreement with the analytical solutions, except for the first part of the graph, which represents only a couple of hundreds of cycles over a total of million cycles. The reason for these differences is that the analytical model does not take into account the formation of the process zone during the initial quasi-static step.

As expected, increasing the mode II displacement, the difference between the value of the local stress ratio and the applied load ratio increases. Furthermore, Fig. 19 also shows how the local stress ratio is not constant with the number of cycles and, for this particular problem, tends to increase as the delamination grows.

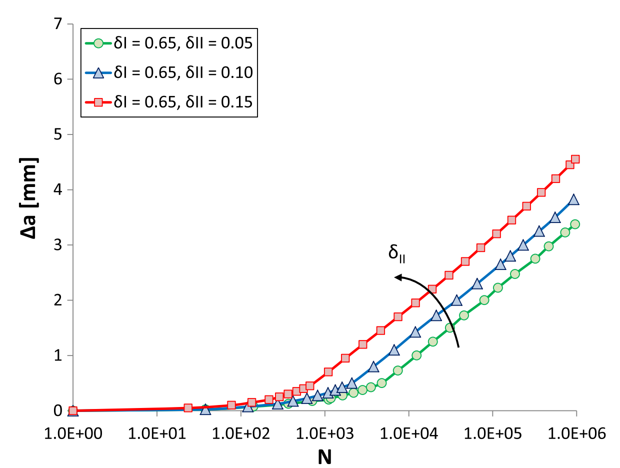

Fig. 15 Fatigue crack growth at different values of applied mode II displacement for modified MMB specimen.

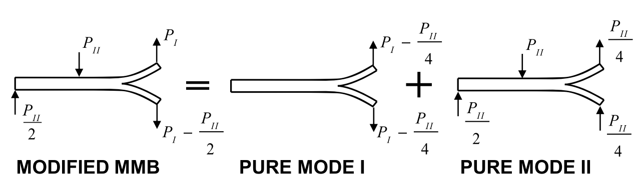

Fig. 16 Modified MMB specimen as a superposition of pure mode I and mode II loadings.

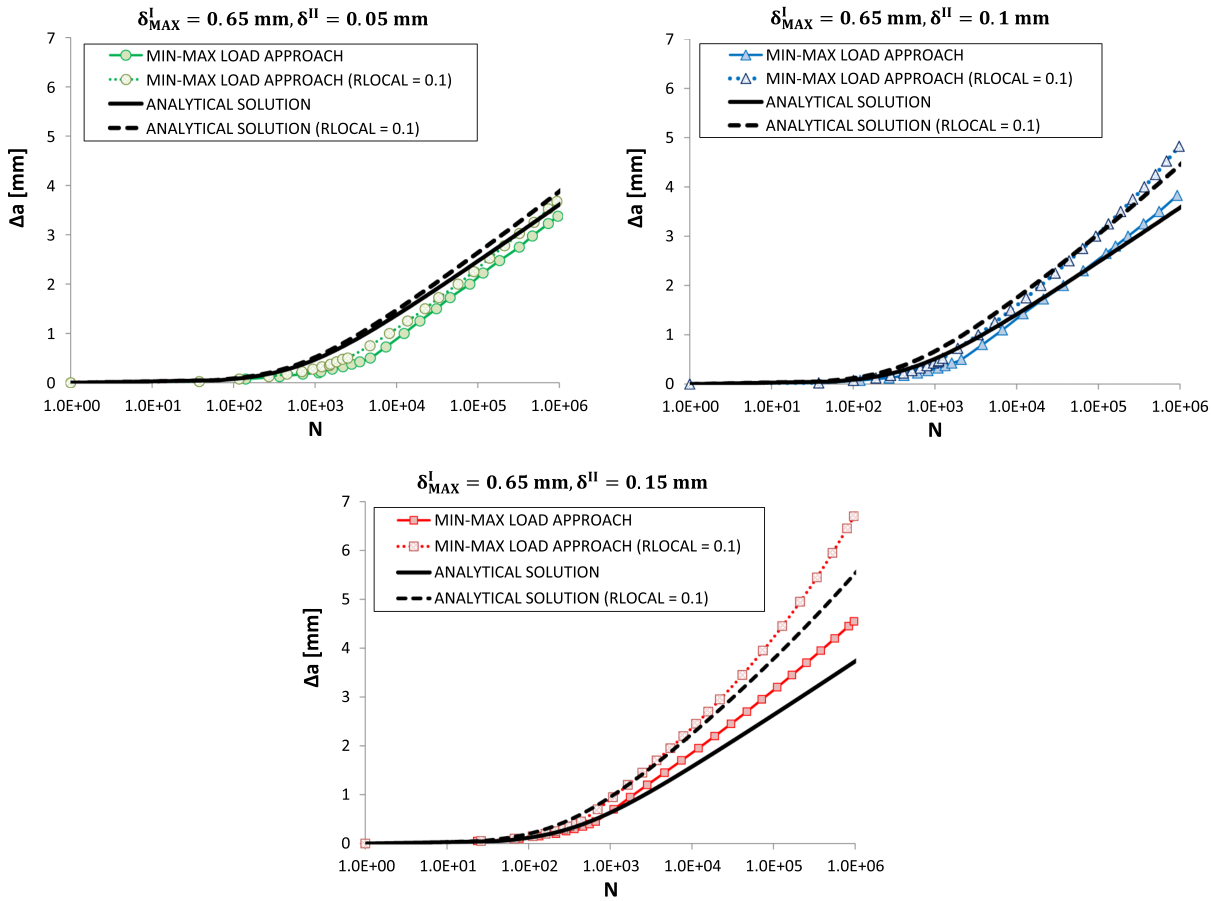

Fig. 17 Comparison of numerical results and analytical solution with and without application of min-max load approach for modified MMB specimen.

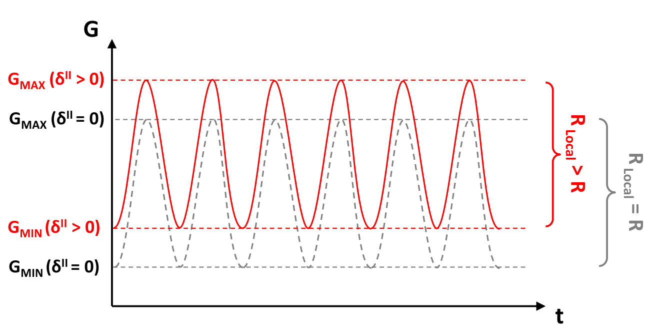

Fig. 18 Difference between applied load ratio and local stress ratio in presence of constant load component.

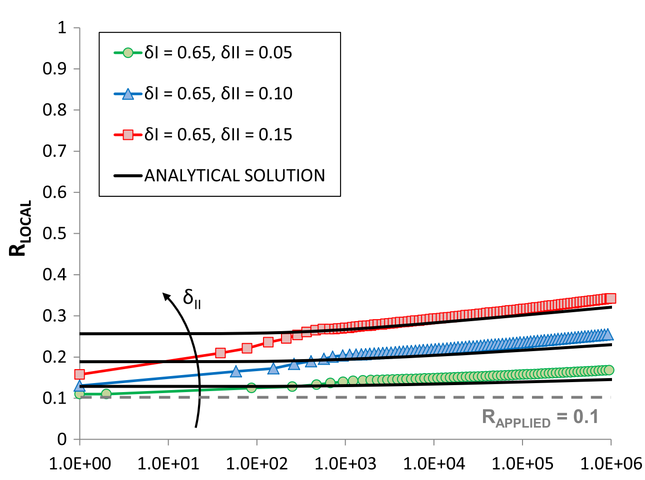

Fig. 19 Comparison of local stress ratio trend for modified MMB specimen.

V. Conclusions

A new strategy for the simulation of fatigue delamination propagation, called min-max load approach, is proposed. The new methodology, based on the cohesive zone model technique, is able to dynamically capture the local stress ratio during the evolution of the damage. A single simulation is performed with two models representing the same structure but with different applied loads. One model represents the deformed shape of the structure when the applied load is equal to the minimum value of the fatigue cycle, and the other one represents the deformed configuration of the structure at the maximum load. Using the minimum and the maximum values of the energy release rate taken from the two models, it is possible to evaluate the local stress ratio. The subroutine UMAT is adopted in ABAQUS to implement the cohesive damage, allowing the two models to communicate with each other exchanging information in terms of energy release rate and damage propagation. The methodology has been validated by performing analyses on double cantilever beam and mixed-mode bending (MMB) specimens. Then, the min-max load approach has been adopted to numerically investigate a specimen equal to the MMB but with modified loading conditions such as to produce a variable local stress ratio different from the applied load ratio. An analytical model based on the corrected beam theory has been employed to validate the outcomes of the numerical simulations. The results of the analyses indicate that the approach is able to correctly predict the fatigue delamination propagation without introducing any information regarding the applied load ratio in the damage constitutive model. Indeed, the local stress ratio is calculated during the analysis, allowing capturing any possible changes of its value along the delamination front and during the delamination evolution.

The work will be extended to other situations where the local stress ratio changes during the delamination evolution, such as the case of a structure subjected to fatigue compressive load in postbuckling regime.

Acknowledgments

This work was sponsored by the Office of Naval Research (ONR), under grant award number N62909-17-1-2129. The views and conclusions contained herein are those of the authors only and should not be interpreted as representing those of ONR, the U.S. Navy, or the U.S. government.

References

[1] Martin, R., "Delamination Fatigue," *Fatigue in Composites*, edited by B. Harris, Woodhead Publishing, Cambridge, England, U.K., 2007, pp. 173–188.
https://doi.org/10.1533/9781855738577.2.173

[2] Sahoo, S. S., Panda, S. K., and Sen, D., "Effect of Delamination on Static and Dynamic Behavior of Laminated Composite Plate," *AIAA Journal*, Vol. 54, No. 8, 2016, pp. 2530–2544.
https://doi.org/10.2514/1.J054908

[3] Paris, P. C., Gomez, M. P., and Anderson, W. E., "A Rational Analytic Theory of Fatigue," *The Trend in Engineering*, Vol. 13, No. 1, 1961, pp. 9–14.

[4] Rans, C., Alderliesten, R., and Benedictus, R., "Misinterpreting the Results: How Similitude Can Improve Our Understanding of Fatigue Delamination Growth," *Composites Science and Technology*, Vol. 71, No. 2, 2011, pp. 230–238.
https://doi.org/10.1016/j.compscitech.2010.11.010

[5] Bak, B., Sarrado, C., Turon, A., and Costa, J., "Delamination Under Fatigue Loads in Composite Laminates: A Review on the Observed Phenomenology and Computational Methods," *Applied Mechanics Reviews*, Vol. 66, No. 6, 2014, pp. 0–24.
https://doi.org/10.1115/1.4027647

[6] Di Memmo, I., and Bisagni, C., "Fatigue Simulation for Damage Propagation in Composite Structures," *Proceedings of 32nd Annual American Society for Composites Technical Conference*, Purdue Univ., West Lafayette, IN, Oct. 2017, pp. 1009–1019.
https://doi.org/10.12783/asc2017/15247

[7] Krueger, R., "Virtual Crack Closure Technique: History, Approach, and Applications," *Applied Mechanics Reviews*, Vol. 57, No. 2, 2004, pp. 109–143.
https://doi.org/10.1115/1.1595677

[8] Krueger, R., "Development of a Benchmark Example for Delamination Fatigue Growth Prediction," NASA CR-2010-216723, 2010.

[9] Krueger, R., "Development and Application of Benchmark Examples for Mixed-Mode I/II Quasi-Static Delamination Propagation Predictions," NASA CR-2012-217562, 2012.

[10] Krueger, R., and Carvalho, N., "In Search of a Time Efficient Approach to Crack and Delamination Growth Predictions in Composites," *Proceedings of 31st ASC Technical Conference*, Vol. 1, Williamsburg, VA, Sept. 2016, pp. 368–383.

[11] Riccio, A., Ronza, F., Sellitto, A., and Scaramuzzino, F., "Modeling Delamination Growth in Composite Panels Subjected to Fatigue Load," *Key Engineering Materials*, Vol. 627, Sept. 2014, pp. 21–24.
https://doi.org/10.4028/www.scientific.net/KEM.627.21

[12] Mabson, G. E., De Carvalho, N. V., and Krueger, R., "VCCT with Progressive Nodal Release for Simulating Mixed-Mode Delamination: Formulation, Algorithmic Improvements and Implications," *Proceedings of 33rd Technical Conference of the American Society for Composites 2018*, Vol. 3, Seattle, WA, Sept. 2018, pp. 1549–1563.
https://doi.org/10.12783/asc33/26029

[13] Bak, B. L. V., Turon, A., Lindgaard, E., and Lund, E., "A Simulation Method for High-Cycle Fatigue-Driven Delamination Using a Cohesive Zone Model," *International Journal of Numerical Methods in Engineering*, Vol. 106, No. 3, 2016, pp. 163–191.
https://doi.org/10.1002/nme.v106.3

[14] Turon, A., Costa, J., Camanho, P. P., and Dávila, C. G., "Simulation of Delamination in Composites Under High-Cycle Fatigue," *Composites Part A: Applied Science and Manufacturing*, Vol. 38, No. 11, 2007, pp. 2270–2282.
https://doi.org/10.1016/j.compositesa.2006.11.009

[15] Pirondi, A., and Moroni, F., "Simulation of Mixed-Mode I/II Fatigue Crack Propagation in Adhesive Joints with a Modified Cohesive Zone Model," *Journal of Adhesion Science and Technology*, Vol. 25, No. 18, 2012, pp. 2483–2499.
https://doi.org/10.1163/016942411X580180

[16] Harper, P. W., and Hallett, S. R., "A Fatigue Degradation Law for Cohesive Interface Elements–Development and Application to Composite Materials," *International Journal of Fatigue*, Vol. 32, No. 11, 2010, pp. 1774–1787.
https://doi.org/10.1016/j.ijfatigue.2010.04.006

[17] Woelke, P. B., Rutner, M. P., Shields, M. D., Rans, C., and Alderliesten, R., "Finite Element Modeling of Fatigue in Fiber-Metal Laminates," *AIAA Journal*, Vol. 53, No. 8, 2015, pp. 2228–2236.
https://doi.org/10.2514/1.J053600

[18] Camanho, P. P., Dávila, C. G., and de Moura, M., "Numerical Simulation of Mixed-Mode Progressive Delamination in Composite Materials," *Journal of Composite Materials*, Vol. 37, No. 16, 2016, pp. 1415–1438.
https://doi.org/10.1177/0021998303034505

[19] Turon, A., Camanho, P. P., Costa, J., and Dávila, C. G., "A Damage Model for the Simulation of Delamination in Advanced Composites Under Variable Mode Loading," *Mechanics of Materials*, Vol. 38, No. 11, 2006, pp. 1072–1089.
https://doi.org/10.1016/j.mechmat.2005.10.003

[20] Kim, E.-H., Lee, I., and Hwang, T.-K., "Low-Velocity Impact and Residual Burst-Pressure Analysis of Cylindrical Composite Pressure Vessels," *AIAA Journal*, Vol. 50, No. 10, 2012, pp. 2180–2193.
https://doi.org/10.2514/1.J051515

[21] Makhecha, D. P., Kapania, R. K., Johnson, E. R., and Dillard, D. A., "Dynamic Fracture Analysis of Adhesively Bonded Joints Using Explicit Methods," *AIAA Journal*, Vol. 45, No. 11, 2007, pp. 2778–2784.
https://doi.org/10.2514/1.26088

[22] Riccio, A., Scaramuzzino, F., and Perugini, P., "Influence of Contact Phenomena on Embedded Delaminations Growth in Composites," *AIAA Journal*, Vol. 41, No. 5, 2003, pp. 933–940.
https://doi.org/10.2514/2.2029

[23] Tzu-Chiang, W., Shih, C. F., and Zhigang, S., "Crack Extension and Kinking in Laminates and Bicrystals," *International Journal of Solids and Structures*, Vol. 29, No. 3, 1992, pp. 327–344.
https://doi.org/10.1016/0020-7683(92)90203-6

[24] Raju, I. S., Crews, J. H., and Aminpour, M. A., "Convergence of Strain Energy Release Rate Components for Edge-Delaminated Composite Laminates," *Engineering Fracture Mechanics*, Vol. 30, No. 3, 1988, pp. 383–396.
https://doi.org/10.1016/0013-7944(88)90196-8

[25] Krueger, R., Deobald, L., Mabson, G. E., Engelstad, S., Rao, M. P., Gurvich, M., Seneviratne, W., Perera, S., O'Brien, T. K., Murri, G., et al., "Guidelines for VCCT-Based Interlaminar Fatigue and Progressive Failure Finite Element Analysis," NASA TM-2017-219663, 2017.

[26] Dávila, C. G., and Bisagni, C., "Fatigue Life and Damage Tolerance of Postbuckled Composite Stiffened Structures with Initial Delamination," *Composite Structures*, Vol. 161, Feb. 2017, pp. 73–84.
https://doi.org/10.1016/j.compstruct.2016.11.033

[27] Dávila, C. G., and Bisagni, C., "Fatigue Life and Damage Tolerance of Postbuckled Composite Stiffened Structures with Indentation Damage," *Journal of Composite Materials*, Vol. 52, No. 7, 2017, pp. 931–943.
https://doi.org/10.1177/0021998317715785

[28] Abaqus, *Abaqus 2017 Analysis User's Manual*, Dassault Systèmes Simulia Corp., Providence, RI, 2017.

[29] Williams, J. G., "The Fracture Mechanics of Delamination Tests," *The Journal of Strain Analysis for Engineering Design*, Vol. 24, No. 4, 2007, pp. 207–214.
https://doi.org/10.1243/03093247V244207

[30] Reeder, J. R., "Refinements to the Mixed-Mode Bending Test for Delamination Toughness," *Journal of Composites, Technology and Research*, Vol. 25, No. 4, 2003, pp. 0–5.
https://doi.org/10.1520/CTR10961J

[31] Allegri, G., Wisnom, M. R., and Hallett, S. R., "A New Semi-Empirical Law for Variable Stress-Ratio and Mixed-Mode Fatigue Delamination Growth," *Composites Part A: Applied Science and Manufacturing*, Vol. 48, May 2013, pp. 192–200.
https://doi.org/10.1016/j.compositesa.2013.01.018

[32] Benzeggagh, M. L., and Kenane, M., "Measurement of Mixed-Mode Delamination Fracture Toughness of Unidirectional Glass/Epoxy Composites with Mixed-Mode Bending Apparatus," *Composites Science and Technology*, Vol. 56, No. 4, 1996, pp. 439–449.
https://doi.org/10.1016/0266-3538(96)00005-X

P. Weaver
Associate Editor